Supporting Information

Cerium-organic framework as alkaline phosphatase mimics: Ce-OH_2 sites in catalytic dephosphorylation

Sudip Bhattacharjee,[a,‡] Tonmoy Chakraborty,[a,‡] and Asim Bhaumik[a,*]

[a]*School of Materials Sciences, Indian Association for the Cultivation of Science, 2A & 2B Raja S. C. Mullick Road, Jadavpur, Kolkata 700032, India.*

Email: msab@iacs.res.in

‡SB and TC contributed equally to this paper.

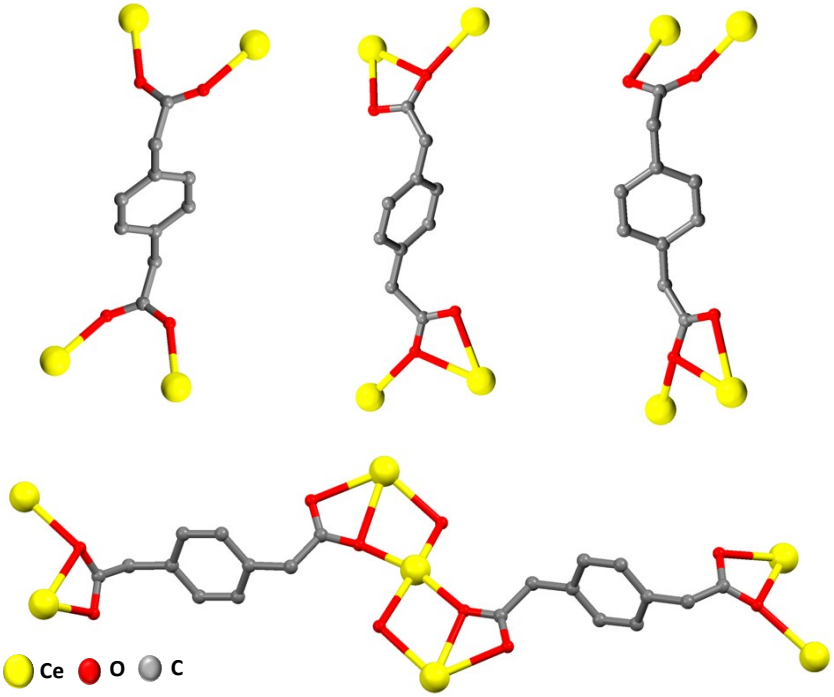

Figure S1. Various coordination mode of PDA ligand with Ce metal.

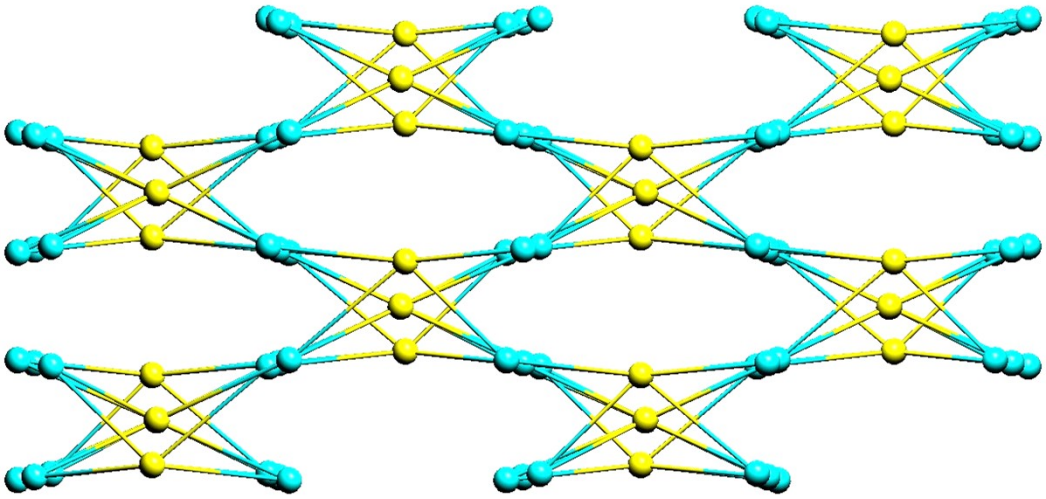

Figure S2. Topological representation of Ce-MOF underlying net 4,4,6,6T3. Ce (yellow) PDA ligand (sky blue).

Table S1. Bond Lengths (Å) for Ce-MOF.

Atom	Atom	Length/Å	Atom	Atom	Length/Å
Ce1	O5	2.391(3)	O13	Ce2[6]	2.514(3)
Ce1	O7	2.426(3)	O11	Ce1[5]	2.477(3)
Ce1	O4	2.434(3)	O13	Ce1[2]	2.682(3)
Ce1	O11[1]	2.477(3)	O3	Ce2[1]	2.583(4)
Ce1	O12[2]	2.517(3)	O2	Ce2[3]	2.524(3)
Ce1	O1[3]	2.522(3)	O2	Ce1[3]	2.704(3)
Ce1	O10[1]	2.655(3)	C25	Ce1[2]	2.982(4)
Ce1	O13[2]	2.683(3)	O12	Ce1[2]	2.517(3)
Ce1	O2[3]	2.704(3)	C8	Ce1[3]	3.002(5)
Ce1	C26[1]	2.944(5)	C26	C27	1.504(6)
Ce1	C25[2]	2.982(4)	C26	Ce1[5]	2.944(5)
Ce1	C8[3]	3.002(5)	O10	Ce1[5]	2.655(3)
Ce2	O9	2.457(4)	O4	Ce2[1]	2.625(3)
Ce2	O10	2.477(3)	O1	Ce1[3]	2.522(3)
Ce2	O6	2.478(3)	Ce2	C10[5]	3.003(5)
Ce2	O13[4]	2.514(3)	Ce2	Ce1[5]	3.9626(4)
Ce2	O2[3]	2.524(3)	C10	Ce2[1]	3.003(5)
Ce2	O7	2.547(3)	Ce2	O4[5]	2.625(3)
Ce2	O3[5]	2.583(4)	Ce2	C16	2.972(5)
Ce2	O8	2.593(4)			

[1]+X,1/2-Y,1/2+Z; [2]-X,1-Y,1-Z; [3]1-X,-Y,1-Z; [4]-X,-1/2+Y,1/2-Z; [5]+X,1/2-Y,-1/2+Z; [6]-X,1/2+Y,1/2-Z; [7]-X,1-Y,-Z; [8]1-X,1-Y,1-Z

Table S2. Bond Angles (˚) for Ce-MOF.

Atom	Atom	Atom	Angle/°	Atom	Atom	Atom	Angle/°
O5	Ce1	O7	86.49(12)	O10	Ce2	$C10^{5}$	77.72(12)
O5	Ce1	O4	81.48(12)	O6	Ce2	$C10^{5}$	97.74(13)
O7	Ce1	O4	166.56(11)	$O13^{4}$	Ce2	$C10^{5}$	92.74(13)
O5	Ce1	$O11^{1}$	158.26(13)	$O2^{3}$	Ce2	$C10^{5}$	82.94(13)
O7	Ce1	$O11^{1}$	76.77(11)	O7	Ce2	$C10^{5}$	151.10(12)
O4	Ce1	$O11^{1}$	116.33(11)	$O3^{5}$	Ce2	$C10^{5}$	24.23(12)
O5	Ce1	$O12^{2}$	77.43(12)	O8	Ce2	$C10^{5}$	154.42(13)
O7	Ce1	$O12^{2}$	72.78(11)	$O4^{5}$	Ce2	$C10^{5}$	25.32(12)
O4	Ce1	$O12^{2}$	110.07(11)	C16	Ce2	$C10^{5}$	169.33(15)
$O11^{1}$	Ce1	$O12^{2}$	84.35(13)	O9	Ce2	$Ce1^{5}$	112.19(10)
O5	Ce1	$O1^{3}$	114.04(12)	O10	Ce2	$Ce1^{5}$	41.12(7)
O7	Ce1	$O1^{3}$	95.52(11)	O6	Ce2	$Ce1^{5}$	157.45(8)
O4	Ce1	$O1^{3}$	84.03(11)	$O13^{4}$	Ce2	$Ce1^{5}$	41.91(7)
$O11^{1}$	Ce1	$O1^{3}$	81.72(13)	$O2^{3}$	Ce2	$Ce1^{5}$	94.81(7)
$O12^{2}$	Ce1	$O1^{3}$	163.59(12)	O7	Ce2	$Ce1^{5}$	119.03(8)
O5	Ce1	$O10^{1}$	146.08(11)	$O3^{5}$	Ce2	$Ce1^{5}$	83.86(8)
O7	Ce1	$O10^{1}$	126.86(10)	O8	Ce2	$Ce1^{5}$	98.78(10)
O4	Ce1	$O10^{1}$	65.90(10)	$O4^{5}$	Ce2	$Ce1^{5}$	36.76(6)
$O11^{1}$	Ce1	$O10^{1}$	50.55(10)	C16	Ce2	$Ce1^{5}$	110.88(10)
$O12^{2}$	Ce1	$O10^{1}$	104.37(10)	$C10^{5}$	Ce2	$Ce1^{5}$	60.22(10)
$O1^{3}$	Ce1	$O10^{1}$	73.07(10)	C8	O2	$Ce2^{3}$	134.7(3)
O5	Ce1	$O13^{2}$	96.07(11)	C8	O2	$Ce1^{3}$	90.8(3)
O7	Ce1	$O13^{2}$	119.65(10)	$Ce2^{3}$	O2	$Ce1^{3}$	105.73(11)
O4	Ce1	$O13^{2}$	67.94(10)	C25	O13	$Ce2^{6}$	167.1(3)
$O11^{1}$	Ce1	$O13^{2}$	80.70(12)	C25	O13	$Ce1^{2}$	90.5(3)
$O12^{2}$	Ce1	$O13^{2}$	49.67(10)	$Ce2^{6}$	O13	$Ce1^{2}$	99.34(11)
$O1^{3}$	Ce1	$O13^{2}$	135.26(10)	C25	O12	$Ce1^{2}$	99.0(3)

O10[1]	Ce1	O13[2]	63.99(10)	C26	O10	Ce2	136.5(3)
O5	Ce1	O2[3]	72.46(11)	C26	O10	Ce1[5]	90.0(3)
O7	Ce1	O2[3]	67.05(10)	Ce2	O10	Ce1[5]	101.04(11)
O4	Ce1	O2[3]	103.32(10)	C10	O4	Ce1	148.0(3)
O11[1]	Ce1	O2[3]	112.32(11)	C10	O4	Ce2[1]	94.0(3)
O12[2]	Ce1	O2[3]	130.47(10)	Ce1	O4	Ce2[1]	103.04(11)
O1[3]	Ce1	O2[3]	49.46(10)	C16	O7	Ce1	150.1(3)
O10[1]	Ce1	O2[3]	122.53(9)	C16	O7	Ce2	96.0(3)
O13[2]	Ce1	O2[3]	166.89(11)	Ce1	O7	Ce2	113.90(12)
O5	Ce1	C26[1]	166.62(12)	C8	O1	Ce1[3]	99.6(3)
O7	Ce1	C26[1]	101.48(12)	C11	O5	Ce1	139.0(3)
O4	Ce1	C26[1]	91.48(12)	C11	O6	Ce2	139.4(3)
O11[1]	Ce1	C26[1]	24.90(12)	C26	O11	Ce1[5]	98.9(3)
O12[2]	Ce1	C26[1]	94.52(12)	C10	O3	Ce2[1]	97.2(3)
O1[3]	Ce1	C26[1]	76.21(12)	C16	O8	Ce2	95.2(3)
O10[1]	Ce1	C26[1]	25.65(11)	O12	C25	O13	119.5(4)
O13[2]	Ce1	C26[1]	70.68(11)	O12	C25	C24	119.9(4)
O2[3]	Ce1	C26[1]	120.47(11)	O13	C25	C24	120.6(4)
O5	Ce1	C25[2]	88.90(13)	O12	C25	Ce1[2]	56.5(2)
O7	Ce1	C25[2]	94.96(11)	O13	C25	Ce1[2]	64.1(2)
O4	Ce1	C25[2]	90.80(11)	C24	C25	Ce1[2]	170.3(3)
O11[1]	Ce1	C25[2]	78.98(13)	O1	C8	O2	120.2(4)
O12[2]	Ce1	C25[2]	24.56(12)	O1	C8	C7	119.0(4)
O1[3]	Ce1	C25[2]	155.27(12)	O2	C8	C7	120.7(4)
O10[1]	Ce1	C25[2]	82.73(12)	O1	C8	Ce1[3]	55.9(2)
O13[2]	Ce1	C25[2]	25.41(11)	O2	C8	Ce1[3]	64.2(2)
O2[3]	Ce1	C25[2]	154.32(11)	C7	C8	Ce1[3]	174.1(3)
C26[1]	Ce1	C25[2]	79.78(13)	O2[3]	Ce2	O4[5]	79.89(10)
O5	Ce1	C8[3]	93.53(13)	O7	Ce2	O4[5]	138.59(11)
O7	Ce1	C8[3]	80.87(12)	O3[5]	Ce2	O4[5]	49.51(10)

O4	Ce1	C8[3]	93.85(11)	O11	C26	Ce1[5]	56.2(2)
O11[1]	Ce1	C8[3]	97.33(13)	O10	C26	Ce1[5]	64.4(2)
O12[2]	Ce1	C8[3]	152.51(12)	C27	C26	Ce1[5]	176.3(3)
O1[3]	Ce1	C8[3]	24.48(12)	O8	Ce2	O4[5]	135.49(12)
O10[1]	Ce1	C8[3]	97.55(12)	O9	Ce2	C16	92.13(15)
O13[2]	Ce1	C8[3]	157.77(12)	O10	Ce2	C16	99.36(12)
O2[3]	Ce1	C8[3]	24.98(11)	O8	C16	Ce2	60.3(3)
C26[1]	Ce1	C8[3]	98.31(13)	O7	C16	Ce2	58.5(2)
C25[2]	Ce1	C8[3]	175.02(12)	C17	C16	Ce2	176.3(3)
O9	Ce2	O10	73.59(12)	O6	Ce2	C16	90.46(13)
O9	Ce2	O6	72.69(13)	O13[4]	Ce2	C16	76.68(13)
O10	Ce2	O6	145.15(11)	O2[3]	Ce2	C16	92.43(12)
O9	Ce2	O13[4]	138.33(13)	O7	Ce2	C16	25.53(12)
O10	Ce2	O13[4]	69.04(11)	O3[5]	Ce2	C16	165.23(13)
O6	Ce2	O13[4]	145.70(11)	O3	C10	Ce2[1]	58.6(3)
O9	Ce2	O2[3]	148.84(12)	O4	C10	Ce2[1]	60.7(2)
O10	Ce2	O2[3]	135.68(10)	C9	C10	Ce2[1]	174.5(4)
O6	Ce2	O2[3]	76.46(11)	O8	Ce2	C16	24.51(12)
O13[4]	Ce2	O2[3]	72.55(11)	O4[5]	Ce2	C16	144.33(12)
O9	Ce2	O7	108.52(14)	O9	Ce2	C10[5]	96.81(16)
O10	Ce2	O7	122.15(10)	O7	Ce2	O8	50.03(10)
O6	Ce2	O7	77.45(11)	O3[5]	Ce2	O8	158.80(15)
O13[4]	Ce2	O7	77.71(11)	O9	Ce2	O4[5]	112.38(13)
O2[3]	Ce2	O7	68.19(10)	O10	Ce2	O4[5]	65.81(10)
O9	Ce2	O3[5]	82.63(15)	O6	Ce2	O4[5]	120.69(11)
O10	Ce2	O3[5]	92.42(12)	O13[4]	Ce2	O4[5]	67.76(10)
O6	Ce2	O3[5]	74.80(11)	O6	Ce2	O8	103.76(13)
O13[4]	Ce2	O3[5]	116.20(11)	O13[4]	Ce2	O8	77.22(14)
O2[3]	Ce2	O3[5]	85.22(13)	O2[3]	Ce2	O8	115.31(12)
O7	Ce2	O3[5]	145.27(12)	O10	Ce2	O8	76.72(11)

O9	Ce2	O8	76.89(16)				

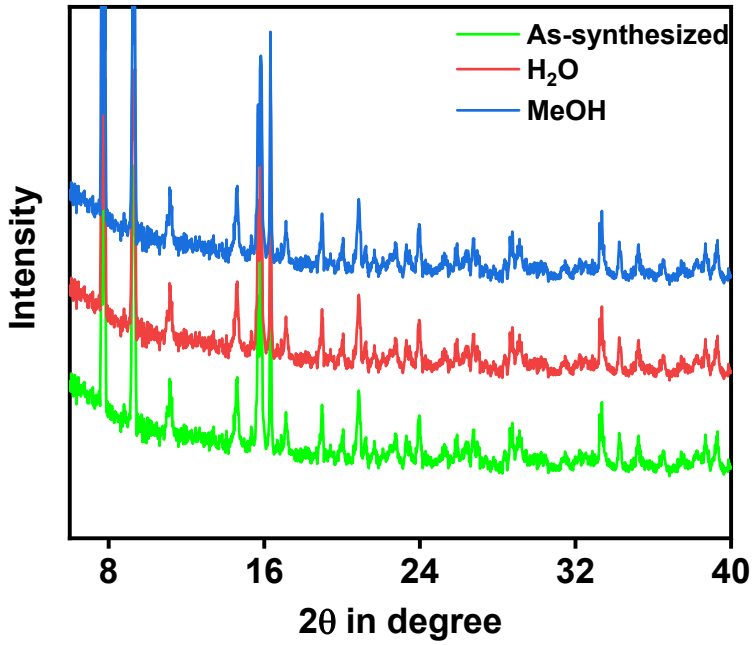

Figure S3. PXRD pattern of Ce-MOF at different solvent medium (soaked for 24 h).

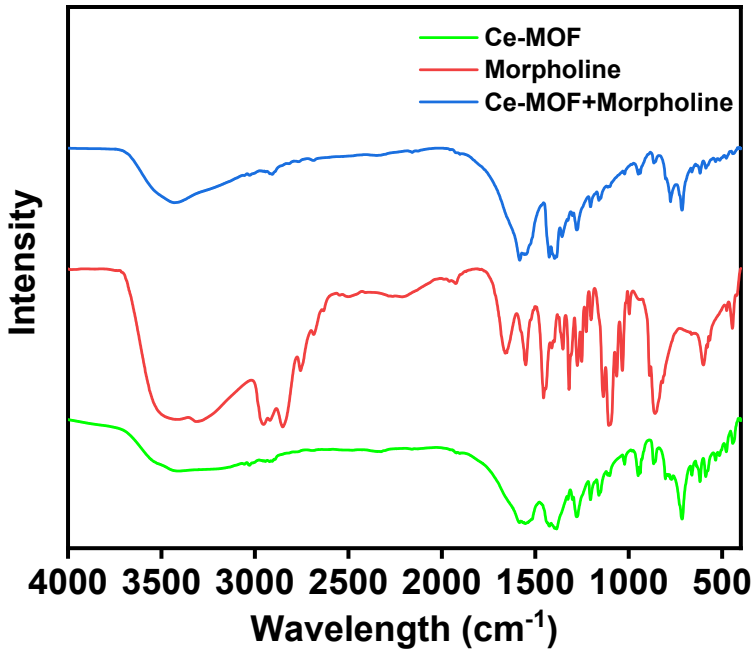

Figure S4. FT-IR of Ce-MOF (without N-Methylmorpholine), N-Methylmorpholine and Ce-MOF (with N-Methylmorpholine) at different solvent medium (soaked for 24 h).

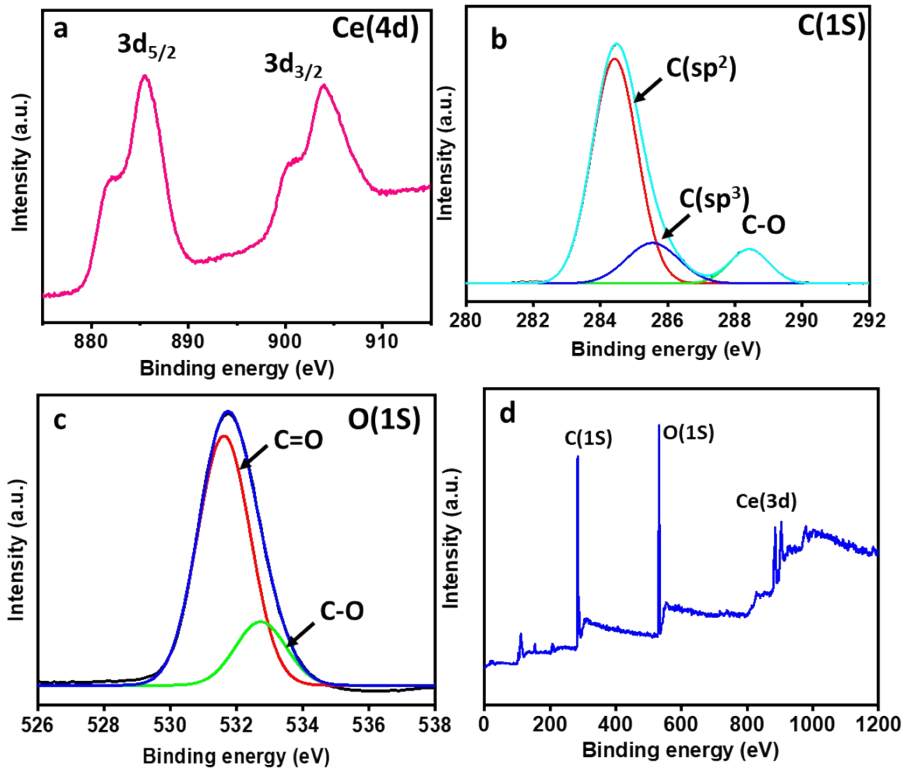

Figure S5. XPS analysis of Ce-MOF.

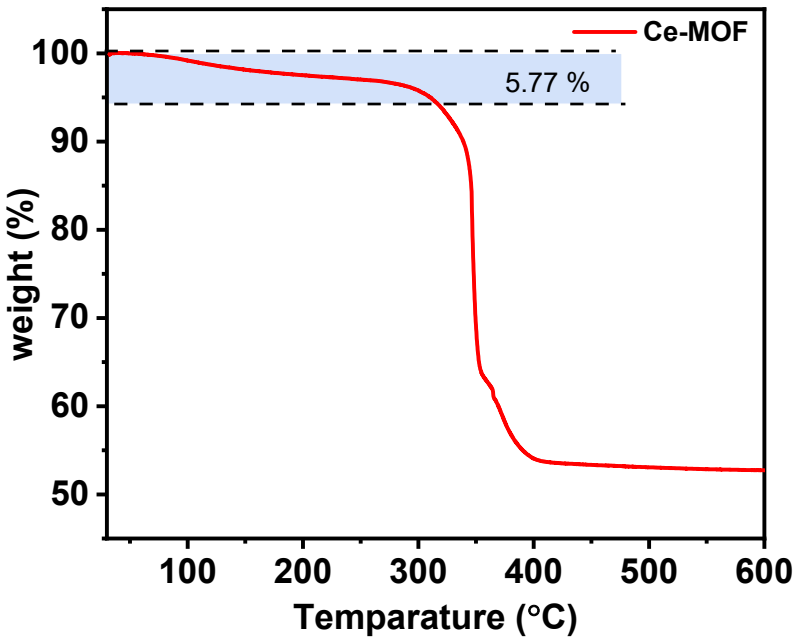

Figure S6. TGA plot of Ce-MOF.

Calculation for weight loss of Ce-MOF:

Formula of asymmetric unit = $C_{30}H_{26}Ce_2O_{13}.2(H_2O)$

Therefore, FW of asymmetric unit = 910 g/mol.

Weight loss for the loss of coordinated and lattice H_2O molecules = (54/910) × 100% = 5.93% (experimental 5.77 %). The further weight loss may be ascribed to the collapse of some additional portion of the polymeric unit of Ce-MOF.

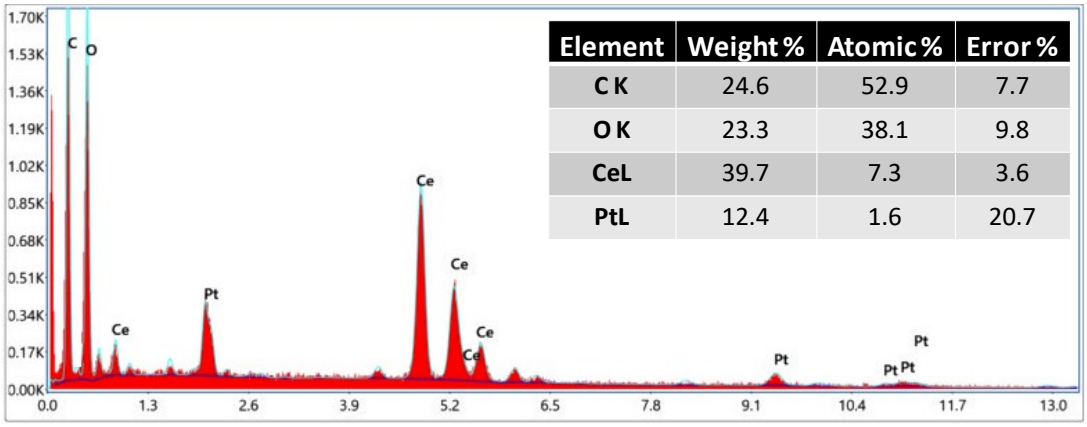

Element	Weight %	Atomic %	Error %
C K	24.6	52.9	7.7
O K	23.3	38.1	9.8
CeL	39.7	7.3	3.6
PtL	12.4	1.6	20.7

Figure S7. Energy dispersive X-ray (EDX) spectrum of Ce-MOF, inset shows the elemental percentage.

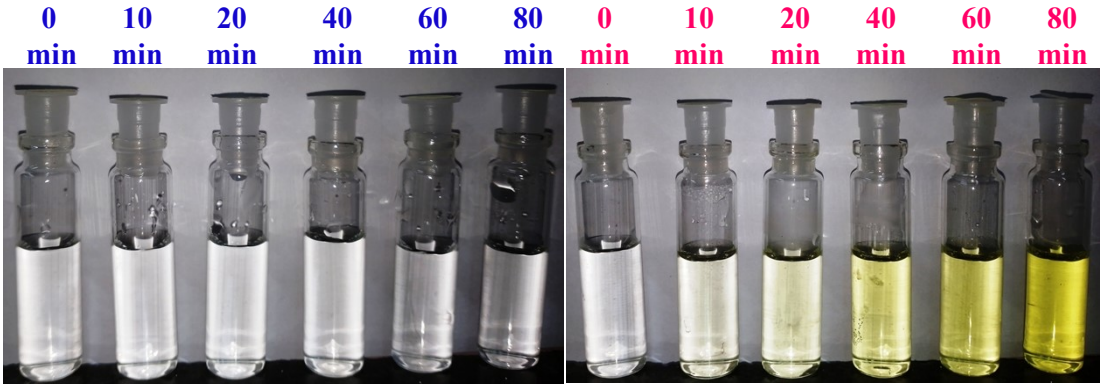

(a) (b)

Figure S8. Color change of 4-NPP hydrolysis reaction over time (a) without catalyst, (b) with catalyst of Ce-MOF.

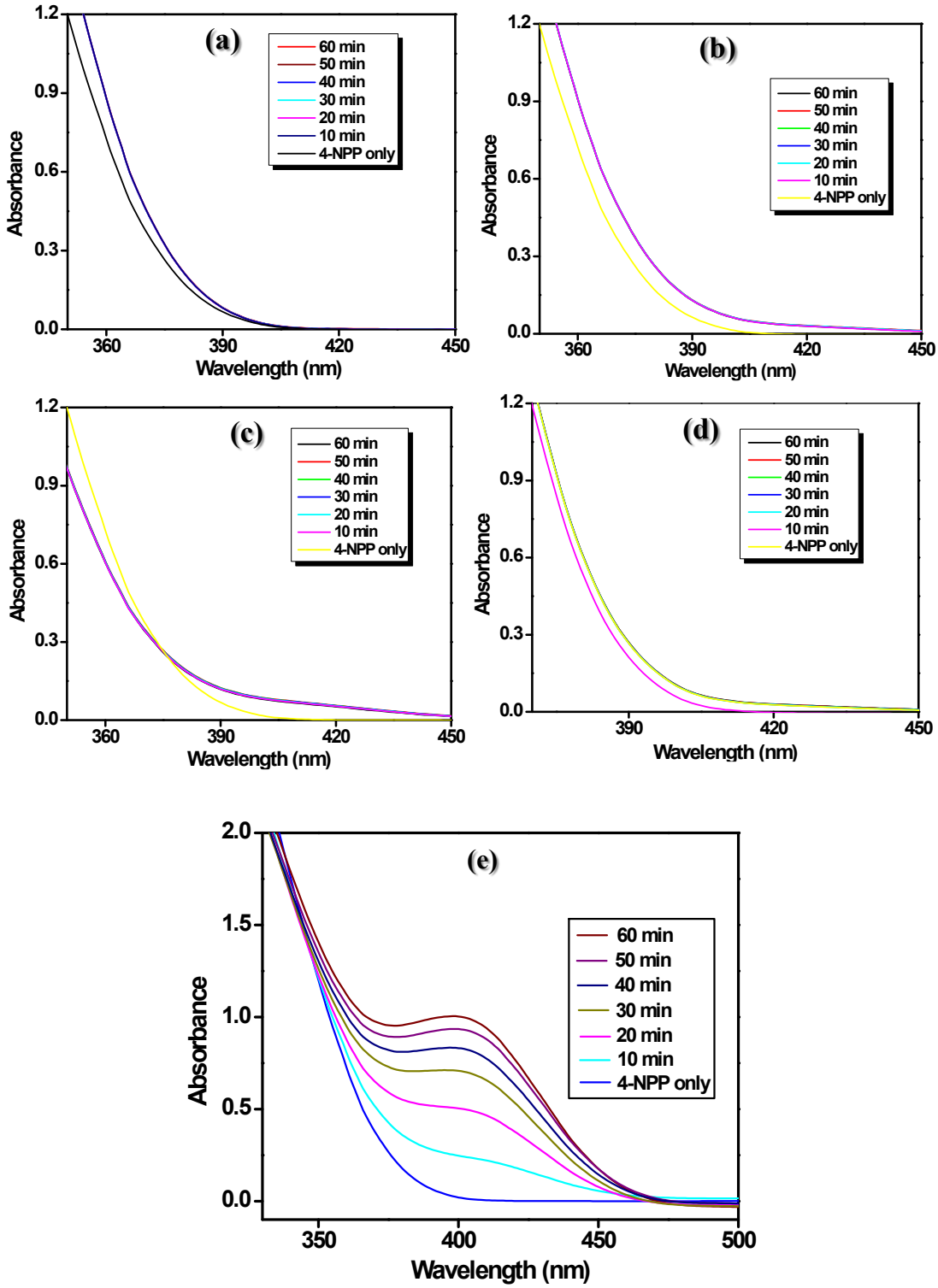

Figure S9. Wavelength scan for the hydrolysis of 4-NPP in the presence of Ce-MOF in (a) H_2O, (b) HEPES buffer (pH 9.0), (c) Tris-HCl buffer (pH 9.0), (d) carbonate buffer (pH 9.0), (e) N-Methylmorpholine buffer (pH 9.0), recorded at 25 °C at intervals of 10 min.

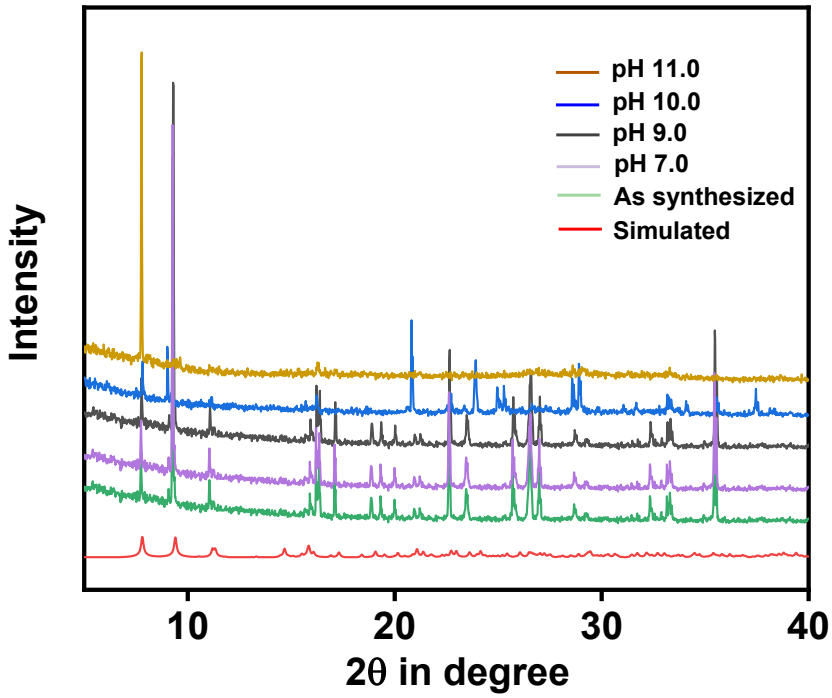

Figure S10. PXRD pattern of Ce-MOF at different pH.

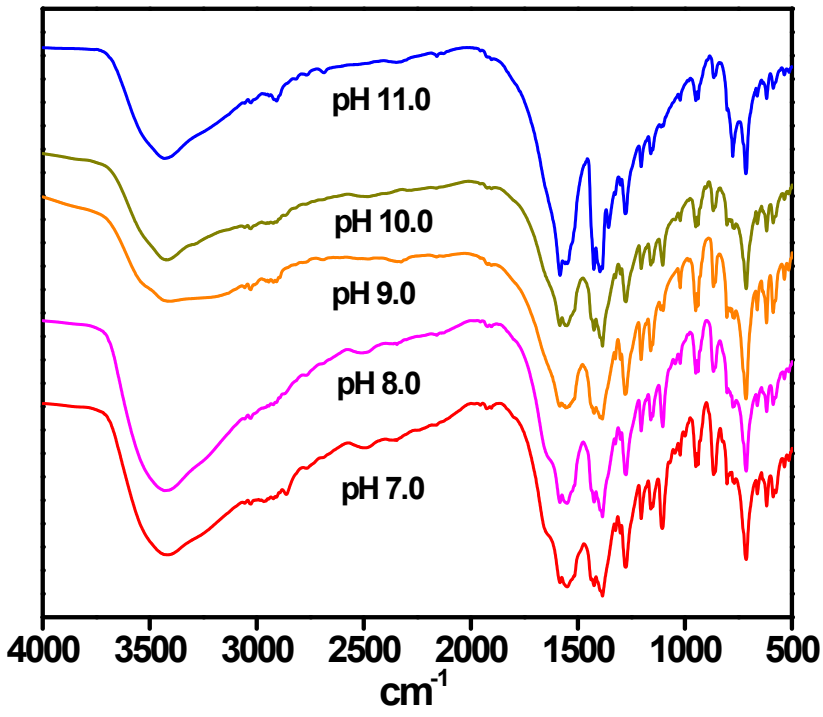

Figure S11. FT-IR spectra of Ce-MOF in different pH medium (N-Methylmorpholine buffered 7.0-11.0).

Table S3. Comparison of hydrolysis rate of p-NPP with various catalysts.

Catalyst	Rate (mM/min^{-1})
Ce-MOF	7.42
$Ce(NO_3)_2.6H_2O$	1.55
PDA	0

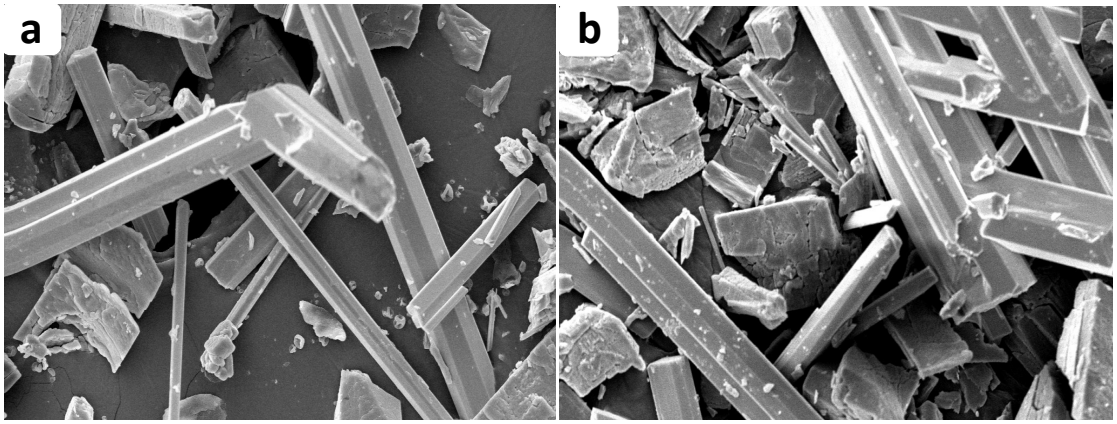

Figure S12. SEM images of Ce-MOF (a) before and (b) after catalysis.

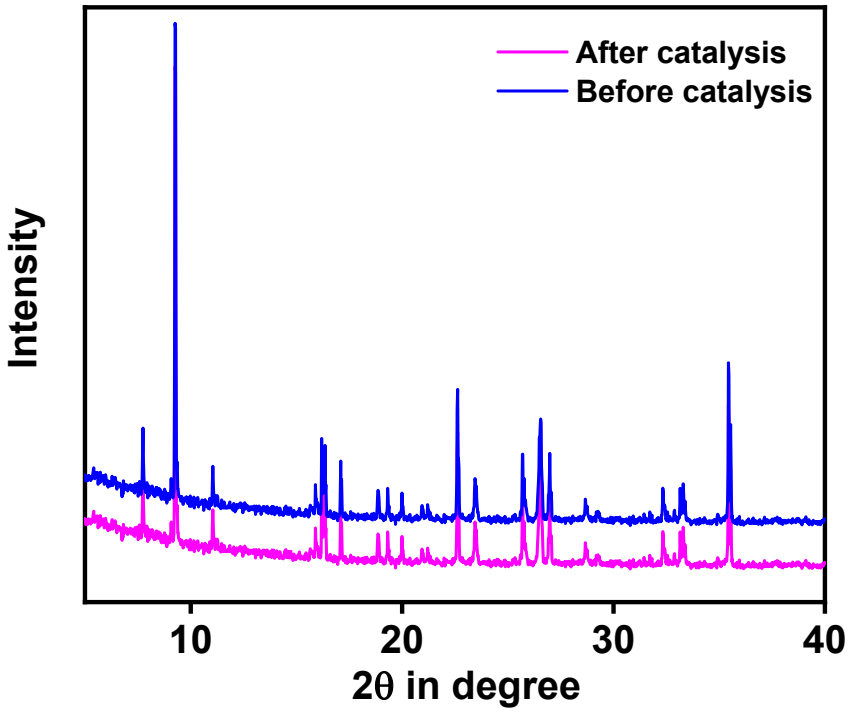

Figure S13. PXRD of Ce-MOF after and before catalysis.

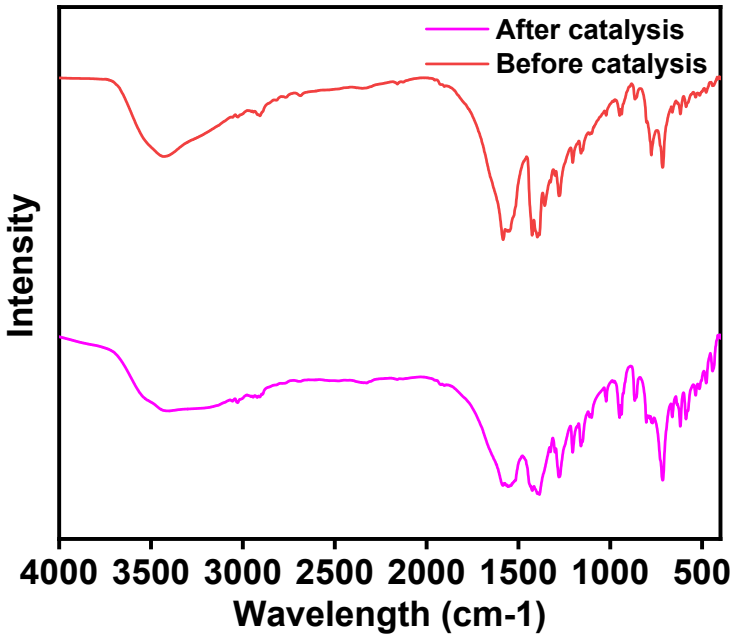

Figure S14. FT-IR of Ce-MOF after and before catalysis.

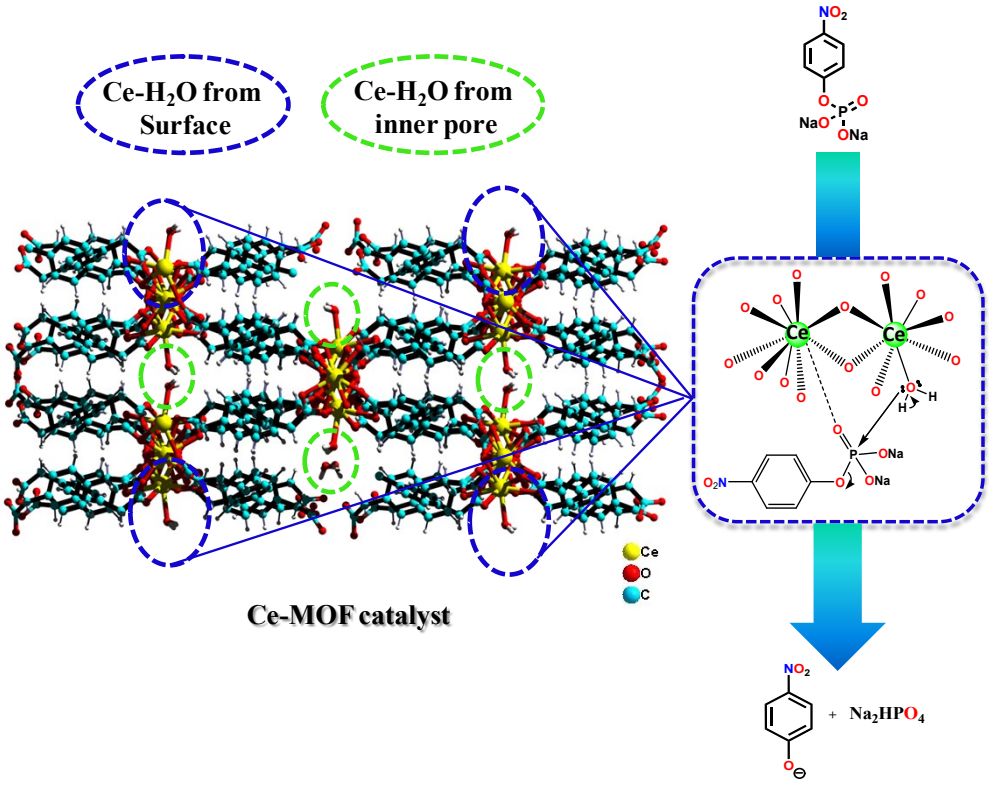

Figure S15. A pictorial diagram of the 4-NPP catalytic hydrolytic reaction with the surface H_2O molecules of the Ce-MOF catalyst.

Table S4. Previously reported K_{cat} values for the hydrolysis of 4-NPP by different catalysts.

Catalyst	Substrate	Solvent	k_{cat}(min^{-1})	Ref.
Hf-Ni	4-NPP	HEPES buffer (pH 7.4)	8.34×10^{-3}	**1**
CeNPs	4-NPP	HEPES buffer (pH 7.0)	2.20×10^{-6}	**2**
Protein Tyrosine Phosphatase	4-NPP	HEPES buffer (pH 7.0)	2.05×10^{3}	**3**
CeCDs	BNPP	Tris-HCl buffer (pH 8.5)	1.84×10^{-3}	**4**
Ce-MOF	**4-NPP**	**N-Methylmorpholine buffer (pH 9.0)**	**7.42×10^{-3}**	**This work**

REFERENCES

1. Dong, J.; An, H. D.; Yue, Z. K.; Hou, S. L.; Chen, Y.; Zhang, Z. J.; & Zhao, B. Dual-Selective Catalysis in Dephosphorylation Tuned by Hf6-Containing Metal–Organic Frameworks Mimicking Phosphatase. *ACS Cent. Sci.,* 2021, **7**, 831-840.
2. Dhall, A.; Burns, A.; Dowding, J.; Das, S.; Seal, S.; and Self, W. Characterizing the phosphatase mimetic activity of cerium oxide nanoparticles and distinguishing its active site from that for catalase mimetic activity using anionic inhibitors. *Environ. Sci. Nano* 2017, **4**, 1742-1749.
3. Wang, S.; Tabernero, L.; Zhang, M.; Harms, E.; Van Etten, R. L.; and Stauffacher, C. V. Crystal structures of a low-molecular weight protein tyrosine phosphatase from Saccharomyces cerevisiae and its complex with the substrate p-nitrophenyl phosphate. *Biochem.,* 2000, **39**, 1903-1914.
4. Du, J.; Qi, S.; Chen, J.; Yang, Y.; Fan, T.; Zhang, P.; and Zhu, C. Fabrication of highly active phosphatase-like fluorescent cerium-doped carbon dots for in situ monitoring the hydrolysis of phosphate diesters. *RSC Adv.,* 2020, **10**, 41551-41559.